Nuclear Physics **A308** (1978) 147–160; © *North-Holland Publishing Co., Amsterdam*

ROTATIONAL STRUCTURES IN DOUBLY ODD TRANSITIONAL Tl NUCLEI †

A. J. KREINER ††, M. FENZL and W. KUTSCHERA

Fachbereich Physik der Technischen Universität München, 8046 Garching, Germany

Received 10 March 1978
(Revised 9 June 1978)

Abstract: The reactions ^{197}Au(α, 5n) at $E_\alpha \approx 65$ MeV and ^{194}Pt(^{6}Li, 4n) at 44 MeV were used to populate high spin states in ^{196}Tl. The subsequent prompt and delayed decay has been studied by means of γ-ray spectroscopic techniques. The strongly Coriolis-distorted $\pi h_{9/2} \otimes \nu i_{13/2}$ two-quasiparticle band found in ^{198}Tl has been followed up to significantly higher angular momenta. All special features displayed by this structure have been interpreted in the framework of a model describing a situation in which two non interacting high-j Nilsson-BCS quasiparticles move in the deformed field of an axially and reflection symmetric rotor. In particular it is shown that the pronounced odd-even staggering of the transition energies can be understood as a specific quantal feature associated with the Coriolis interaction.

E | NUCLEAR REACTIONS ^{197}Au(α, 5nγ), $E \approx 55$–65 MeV, ^{194}Pt(^{6}Li, 4nγ), $E \approx 44$ MeV, measured E_γ, I_γ, $\sigma(E_\alpha, E_\gamma, \theta_\gamma, t)$, γγ-coin, Xγ-coin. ^{196}Tl deduced levels, J, π, $T_{1/2}$, γ-mixing. Enriched target. Ge(Li) detectors.

1. Introduction

The transitional region below lead has been studied quite intensively in recent years, both experimentally and theoretically [1–11]). As a result, evidence has been accumulated which indicates that Hg and Tl nuclei are able to support (at least in some specific families of states) a small and essentially oblate deformation. So-called strongly coupled $h_{\frac{9}{2}}$ proton bands and rotation-aligned $i_{\frac{13}{2}}$ neutron bands have been identified in odd Tl and Hg isotopes respectively [1, 2, 4, 9]). In addition the ground-state bands (g.s.b.) of even Hg nuclei have been established up to spins as high as 20^+ in some cases [11]). The rotational alignment model [12]) seems to provide also in this case an appropriate tool to understand the irregularities of these g.s.b. [ref. [13])]. The compression of the transition energies around spin values 8^+ and 10^+ has been indeed interpreted as arising from the decoupling of a pair of $h_{\frac{9}{2}}$ proton holes [10, 11, 13]).

† This work was partly supported by the DAAD (Deutscher Akademischer Austauschdienst).

†† Present address: Departamento de Física, CNEA, Libertador 8250, Buenos Aires, Argentina.

Hence it appears that the high-j unique parity single-particle states $\pi h_{\frac{9}{2}}$, $\pi h_{\frac{11}{2}}$ and $\nu i_{\frac{13}{2}}$ lying near to the Fermi surface and the collective rotational mode offer the necessary building blocks to correlate a large amount of experimental material. As a nice confirmation of this idea a band displaying collective features based on the $\tilde{\pi}h_{\frac{9}{2}} \otimes \tilde{\nu}i_{\frac{13}{2}}$ intrinsic configuration has been recently reported in the doubly odd nucleus ^{198}Tl [ref. [14])]. In the present work our knowledge about this structure has been extended to considerably higher spins. Due to the larger angular momentum brought into the compound system we succeed in observing the band up to the region where a structural change occurs. Apparently the discontinuity present in the g.s.b. of the core nucleus reflects itself in the yrast band of the neighbouring nuclei producing a similar feature. This phenomenon has already been observed in odd Hg [ref. [11])] and recently also in odd Tl [refs. [8,9])]. This behaviour and also other special features are discussed here in the framework of a model of two non-interacting quasiparticles moving in the deformed field of an axially symmetric rotor [14]).

2. Experimental procedures and results

The present experimental information was obtained in two laboratories with two different accelerators. The reaction ^{197}Au(α, 5n) has been studied first. The α-particle beam was delivered by the isochronous cyclotron at Jülich. In addition, ^{196}Tl was produced using the ^{194}Pt(^{6}Li, 4n) reaction at the MP tandem in Munich. Details about the employed techniques are given for instance in ref. [14]).

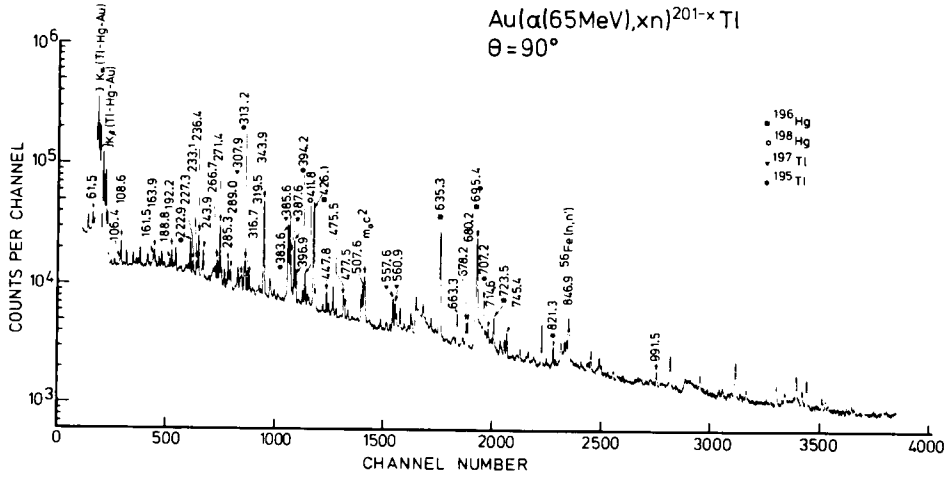

Fig. 1. Singles γ-ray spectrum from the ^{197}Au(α, xn)$^{201-x}$Tl reaction. Lines labelled only by their energies represent transitions in ^{196}Tl.

2.1. SINGLES MEASUREMENTS

In order to select the most adequate beam energy to populate states in ^{196}Tl, an excitation function for the ^{197}Au(α, 5n) reaction was obtained covering the bombarding energy range $E_\alpha \approx$ 55–65 MeV in steps of 5 MeV. For the further investigation the highest beam energy was selected even when the 6n channel begins to

TABLE 1

Transition energies in ^{196}Tl, angle integrated γ-intensities and angular distribution coefficients in the ^{197}Au(α, 5n) reaction at $E_\alpha \approx$ 65 MeV

E_γ [a] (keV)	I_γ [b]	A_2/A_0	A_4/A_0	$\delta(\delta_{min}; \delta_{max})$	Type
61.5	8.0	−0.54±0.10	0.01 ±0.01	−0.18(−0.25; −0.04)	$I \rightarrow I-1$
106.4	1.8	−0.36±0.06	0.001±0.002	−0.07(−0.10; −0.03)	$I \rightarrow I-1$
108.6	8.9	−0.34±0.02	0.001±0.001	−0.05(−0.07; −0.04)	$I \rightarrow I-1$
161.5	4.0	−0.32±0.02	0.09 ±0.08	−0.16(−3.00; −0.10)	$I \rightarrow I-1$
163.5	6.5	−0.37±0.03	0.07 ±0.06	−0.25(−0.32; −0.20)	$I \rightarrow I-1$
188.8	3.4	−0.39±0.04	0.004±0.003	−0.12(−0.16; −0.08)	$I \rightarrow I-1$
192.2	7.7	−0.36±0.03	0.007±0.006	−0.78(−1.48; −0.55)	$I \rightarrow I-1$
227.3	4.8	−0.14±0.10	0.00 ±0.01	0.00(−0.10; 0.10)	$I \rightarrow I-1$
233.1	5.1	−0.35±0.05	0.004±0.002	−0.27(−0.34; −0.19)	$I \rightarrow I-1$
236.4	18.4	−0.39±0.03	0.01 ±0.01	−0.44(−0.55; −0.36)	$I \rightarrow I-1$
243.9	14.1	0.14±0.02	0.04 ±0.05		
266.7	7.0	−0.48±0.03	0.01 ±0.01	−0.31(−0.38; −0.23)	$I \rightarrow I-1$
271.4	30.2	−0.44±0.04	0.01 ±0.01	−0.45(−0.70; −0.35)	$I \rightarrow I-1$
285.3	11.4	−0.36±0.04	0.002±0.001	−0.07(−0.09; −0.05)	$I \rightarrow I-1$
289.0	7.8	−0.35±0.05	0.005±0.005	−0.46(−0.67; −0.30)	$I \rightarrow I-1$
316.7	4.7	−0.54±0.05	0.011±0.008	−0.18(−0.21; −0.14)	$I \rightarrow I-1$
319.5	6.4	−0.53±0.05	0.02 ±0.02	−0.78(−1.43; −0.60)	$I \rightarrow I-1$
336.2	2.9	−0.47±0.08	0.007±0.006	−0.14(−0.19; −0.09)	$I \rightarrow I-1$
343.9	87.4	−0.21±0.02	0.005±0.007	−0.14(−0.21; −0.10)	$I \rightarrow I-1$
380.3	2.1	0.14±0.01	−0.01 ±0.01		
394.2 [c]	33.5	−0.69±0.07	0.05 ±0.03	−0.81(−0.90; −0.70)	$I \rightarrow I-1$
396.9	13.5	−0.53±0.02	0.02 ±0.01	−0.62(−0.85; −0.53)	$I \rightarrow I-1$
447.8	7.7	−0.57±0.04	0.02 ±0.01	−0.55(−0.67; −0.49)	$I \rightarrow I-1$
451.3	3.2	−0.78±0.10	0.05 ±0.05	−0.60(−1.88; −0.42)	$I \rightarrow I-1$
475.3	7.3	−0.83±0.07	0.11 ±0.08	−1.11(−1.48; −0.55)	$I \rightarrow I-1$
507.6	10.7	0.22±0.02	−0.03 ±0.02		
633.3	5.5	0.34±0.03	−0.10 ±0.08		
663.3	16.3	0.25±0.02	−0.04 ±0.04		
678.2	9.1	0.17±0.02	0.02 ±0.03		
680.6	11.4	0.33±0.02	−0.09 ±0.08		
714.6	7.0	0.27±0.04	−0.06 ±0.04		
721.0	3.2	0.28±0.06	−0.06 ±0.05		
745.3	10.7	0.23±0.03	−0.04 ±0.04		
991.5	4.5	0.45±0.09	0.05 ±0.04		

The mixing ratio and the type of transition are as extracted from a $\chi(\delta)$ analysis.

[a]) $0.2 \leqq \Delta E_\gamma \leqq 0.3$ keV.

[b]) Errors range from 5 % to 15 % (for the weakest lines).

[c]) Transition in ^{195}Tl.

compete in order to shift the population distribution in the residual nucleus to larger spin values. Fig. 1 shows an in-beam γ-ray single spectrum. Due to the relatively high excitation energy of the compound system the cross sections for the different exit channels are broad and we see therefore contributions from the neighbouring odd mass Tl isotopes. In addition, with the target in saturation, the decay of the formed activities was followed over several periods of ^{196m}Tl. To determine the angular distribution of the emitted radiation, spectra at six different angles between 90° and 165° (with respect to the beam direction) were measured. Table 1 displays the results of this measurement for those γ-rays which most likely belong to ^{196}Tl. For spin assignments and to extract quadrupole-dipole mixing ratios a $\chi^2(\delta)$ analysis of the data was performed. These results are listed only for those lines for which such a procedure gives a conclusive answer. Fig. 2 illustrates the method for the 108.6 keV dipole type transition. Clearly, the only acceptable solution is the stretched $L = 1$. However, the uncertainty interval for δ is probably somewhat larger than that lying below the 0.1 % confidence limit because the position of the minima depends sensitively on the normalization.

2.2. COINCIDENCE MEASUREMENTS

The first coincidence run was performed using the ^{197}Au(α, 5n) reaction. Conventional four parameter E_{γ_1}-E_{γ_2}-$t_{\gamma_1\gamma_2}$-$t_{\gamma_1\text{r.f.}}$ (energies of the two γ-quanta, time between them and time interval between the arrival of γ_1 and the radio-frequency signal) were recorded event by event on magnetic tape and sorted off-line. From these measurements three different families of γ-rays have been identified. Figs. 3 and 4 display such coincidence spectra for nearly all members of the strongest cascade ending at the 21 ns isomeric state. A coincidence efficiency calibration for the set-up was

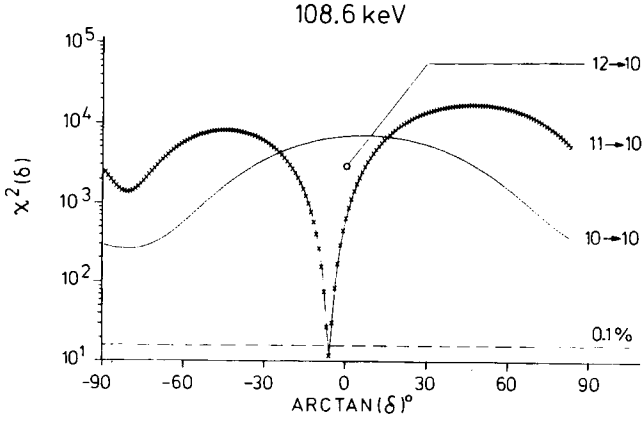

Fig. 2. The χ^2 of the fits for the different possibihties are plotted as a function of the quadrupole-dipole mixing ratio (δ).

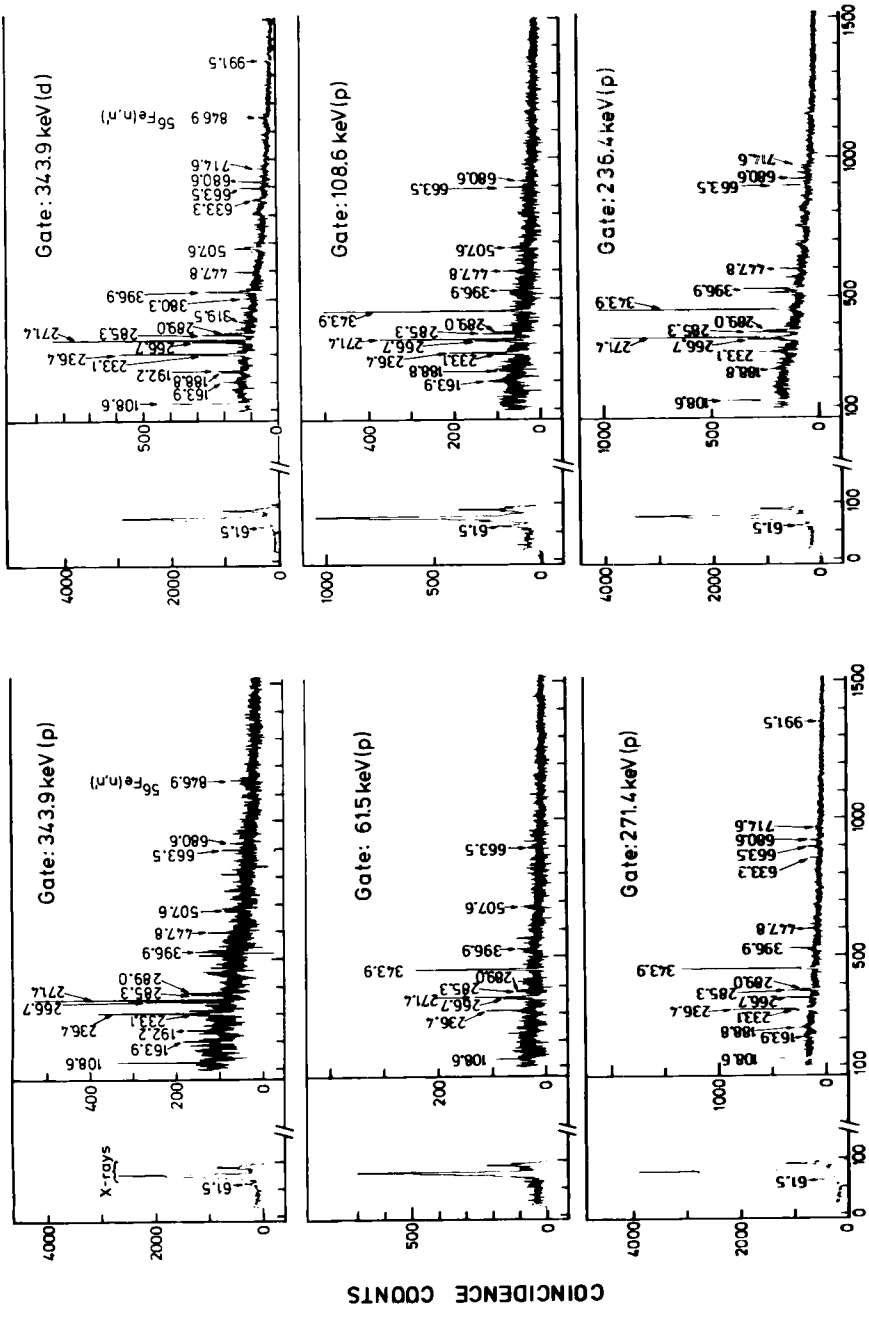

Fig. 3. Some γ-γ coincidence spectra obtained by gating several lines of the main cascade in ^{196}Tl. Here p stands for prompt events and d indicates a delayed time window.

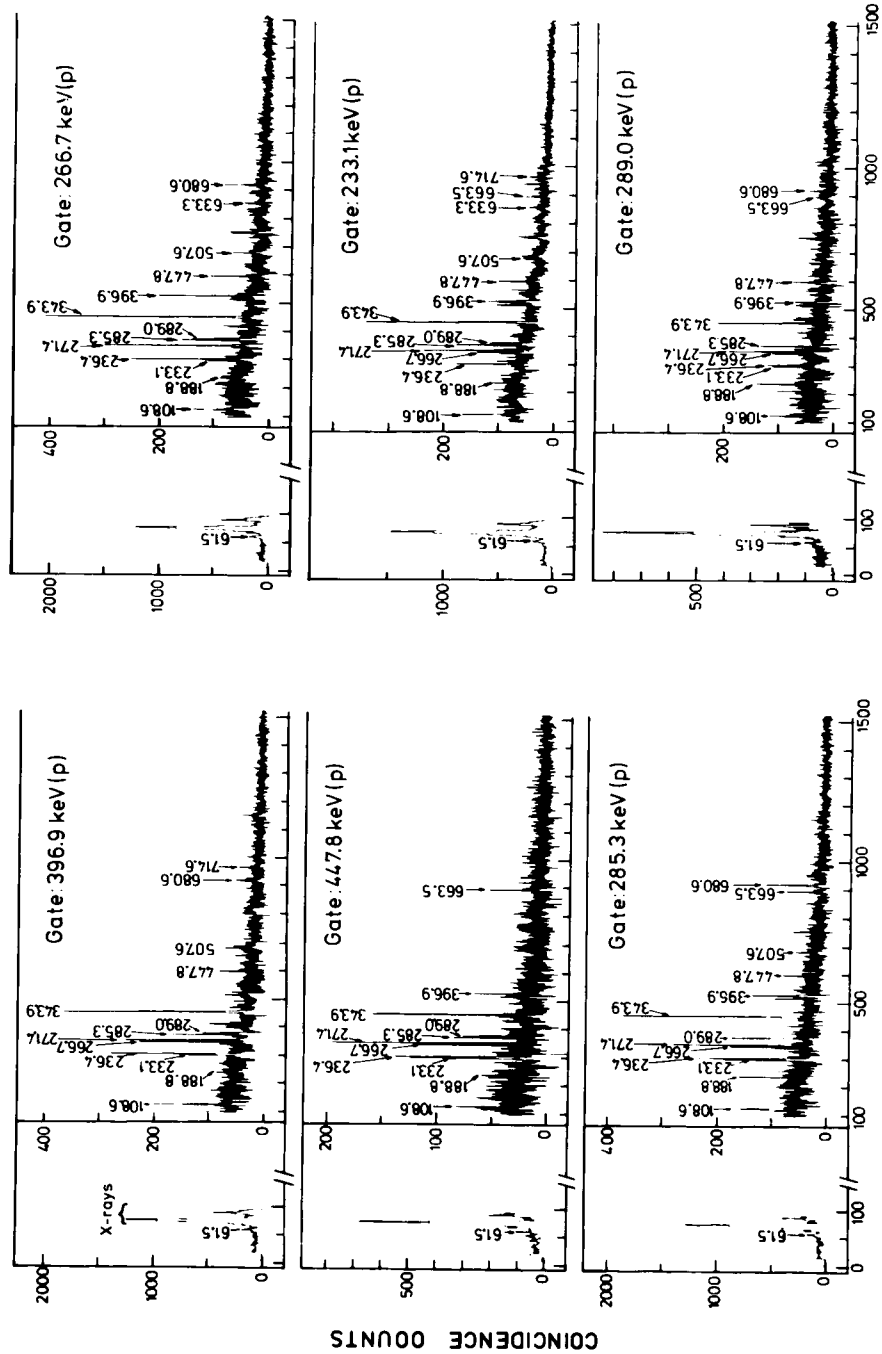

Fig. 4. Additional γ-γ coincidence spectra generated by setting gates on the higher members of the negative-parity cascade.

obtained with known radioactive sources in order to do a quantitative evaluation of the intensities in coincidence with the different γ-ray energy gates. This analysis provides strong arguments for the construction of the levels. An additional X-γ coincidence experiment was performed to investigate the γ-ray energy region below $\approx$ 80 keV using the ^{194}Pt(^{6}Li, 4n) reaction at 44 MeV. An 83 % enriched ^{194}Pt 7 mg/cm^2 target was irradiated with a completely stripped ^{6}Li beam at 11 MV tandem terminal voltage.

In normal coincidence experiments performed with large Ge(Li) detectors it is difficult to achieve a good time resolution for small γ-ray energies. In order to prevent noise triggering of the fast time derivation circuitry, low energies are usually so much handicapped that they may easily get lost. Indeed, we believe that this has been the cause for the non-observation of the analog to the 61.5 keV γ-ray in ^{198}Tl [ref. [14])]. For this reason a three parameter coincidence (E_{γ_1}-E_{γ_2}-$t_{\gamma_1\gamma_2}$) between a very large Ge(Li) detector (140 cm^3, 27 % efficiency) and a planar intrinsic Ge spectrometer (10 cm^3) was measured. A summed coincidence spectrum is shown in fig. 5 (added gates: 343.9, 271.4 and (236.4+233.1) keV). This measurement confirms the existence of the 61.5 keV line and sets an experimental upper limit for the energy of other γ-rays. We give in table 2 the total transition intensities in coincidence for the gates added up in fig. 5.

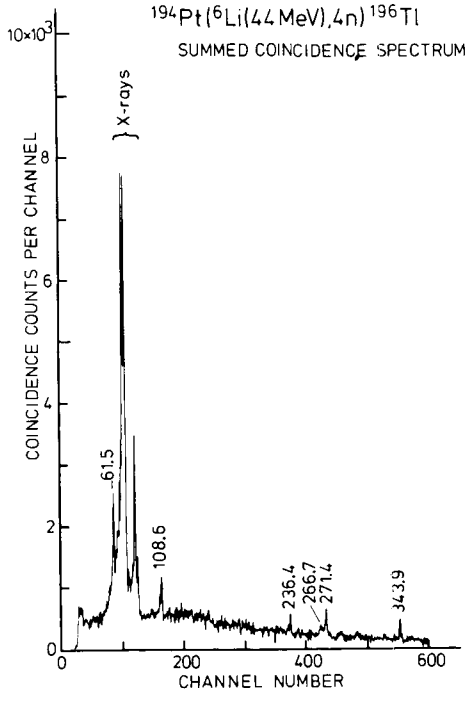

Fig. 5. Summed coincidence spectrum as viewed by a planar detector.

TABLE 2

Total transition coincidence intensities for three of the largest gates in the negative-parity cascade

Gate energy (keV) \ E_γ	61.5	108.6	271.4	236.4	266.7	343.9
343.9	56±4	33±3	19±2	10±1	5±1	
271.4	28±3	28±3		17±2		15±2
236.4+233.1	44±4	37±4	31±3			26±3

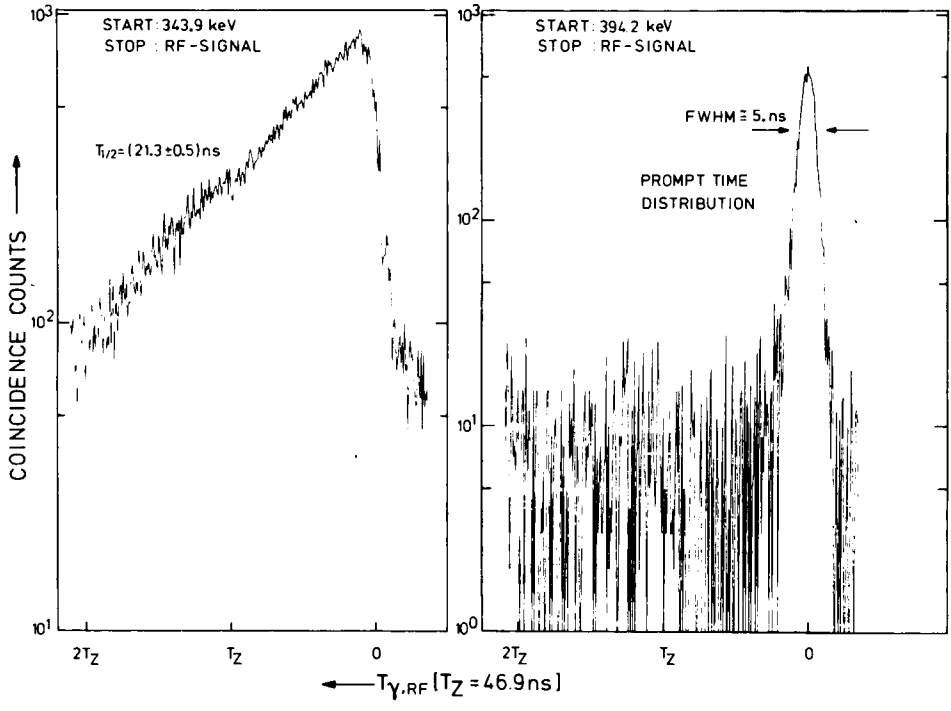

Fig. 6. The time distributions of two different γ-rays. The narrow one at the right illustrates the time resolution of the setup (corresponds to the $\frac{11}{2}^- \rightarrow \frac{9}{2}^-$ transition in ^{195}Tl, refs. [2,8]).

In order to search for ns isomerism a two parameter coincidence (E_γ-$t_{\gamma r.f.}$) was measured which allows us to determine time distributions of the γ-rays with respect to the beam burst.

Using a small 10 cm^3 Ge(Li) detector a time resolution of $\approx$ 5 ns for $E_\gamma \approx$ 350 keV could be achieved. The natural time structure of the cyclotron was expanded suppressing two thirds of the bursts, giving a resulting "silence" period of 141 ns [ref. [15])]. Fig. 6 displays the time distribution obtained for the 343.9 keV isomeric transition and a prompt time curve for reference purposes.

3. The level scheme

Our preceding knowledge about ^{196}Tl was restricted to a few low spin states populated by electron capture decay of ^{196g}Pb and to the decay scheme of a long-lived 7^+ isomeric state ($T_{\frac{1}{2}} = 1.41$ h). None of the low spin states are populated in-beam in our case. The 7^+ state decays with a branching of 96.2 % to ^{196}Hg [ref. [16])] and represents for us an effective ground state. The consistency of building up structures on it has been checked making an intensity balance between prompt population and ^{196}Hg activity lines. The new level scheme proposed here is shown in fig. 7. Three different cascades have been identified. We only want to discuss in some detail the band on top of the 8^- isomer; the arguments used for the other parts of the scheme are of similar nature.

The 343.9 keV line is the strongest one in the spectrum and is in delayed coincidence

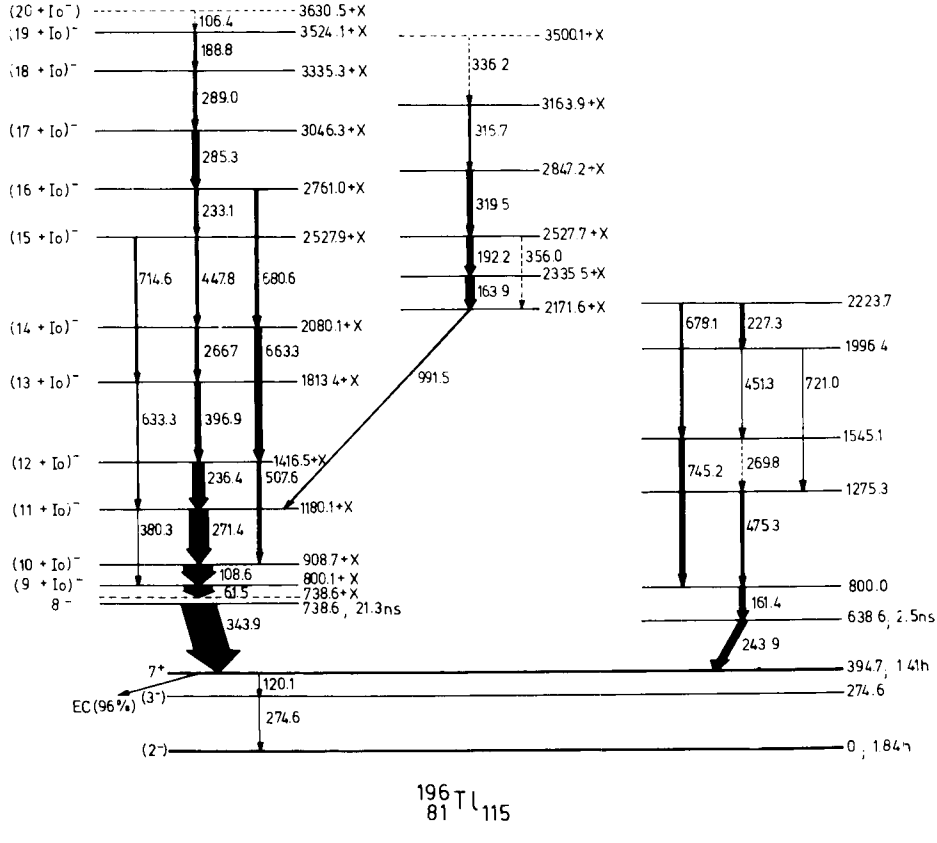

Fig. 7. Level scheme proposed in the present work. The arrow widths for transitions in the negative-parity band are proportional to the total transition intensities. For the other parts they just reflect the γ-intensities. See also text.

with all the other members of the cascade. These facts firmly establish an isomeric state at 738.6 keV as the band head. The part of the band starting from the $(9+I_0)^-$ state up to the $(19+I_0)^-$ state is almost surely established by: (i) a careful quantitative evaluation of the relative intensities in coincidence with the different gating energies, and (ii) the existence of the crossover transitions in coincidence spectra (for the states up to $I^\pi = (16+I_0)^-$). To illustrate the procedure some of these figures are given in table 2 for the second coincidence experiment. The only apparent inconsistency is the too-low intensity of the 343.9 line. However, this is connected with its lifetime; part of the intensity lies outside the accepted time window for prompt events. The placement of the 61.5 keV transition follows also from coincidence intensity arguments. Additional support would come from the 108.6 + 61.5 keV cross over transition but its non-appearance is expected. If the B(E2)/B(M1) branching is borrowed from the $(11+I_0)^-$ state (which actually represents an upper limit because this ratio is decreasing band down) the calculated intensity of the 108.6 + 61.5 keV E2 γ-ray lies well below the experimental limit.

The fact that the negative-parity band starts with such small transition energies seems to suggest especial caution in assigning the 61.5 keV γ-ray as the first intraband transition. Indeed, it cannot be decided as a consequence of our measurements if there are other unobserved cascade transitions and therefore spins and level energies remain uncertain to some extent. These low energy lines represent a general problem in γ-ray spectroscopy, especially on complex heavy nuclei. Due to the strong conversion the deexcitation will no longer proceed through γ-emission below a certain transition energy (assuming that the intraband $\Delta L = 1$ lines are of M1 character). At least, from our X-γ coincidence experiment we can put an upper limit of about 35 keV for the unobserved energy (here the total conversion coefficient already amounts $\approx$ 34). The possibility of measuring conversion electrons turns out to be very difficult because of the extremely large δ-ray background present in-beam. Therefore the definitive clarification of this point remains a challenging experimental problem.

The parity of the band has been concluded from a comparison with the analogous structure in ^{198}Tl. The B(E1) values for the transitions depopulating the 8^- states in both nuclei are in fact very similar (B(E1) = $(0.58 \pm 0.02) \times 10^{-6}$ and $(0.49 \pm 0.02) \times 10^{-6}$ $(e \cdot \mathrm{fm})^2$ for ^{198}Tl and ^{196}Tl respectively).

4. Discussion and conclusions

The discussion will be concerned with the negative-parity band. The gross features of the analogous structure in ^{198}Tl has been already successfully analyzed in terms of the particle-plus-rotor model [14]). The aim of the present work is therefore to understand fmer details of these bands. A more comprehensive study of the model-parameter space enables us to give a physically transparent picture of the structural changes we believe are occurring in the yrast states of ^{196,198}Tl.

Similar two-quasiparticle-plus-rotor calculations have been already done in the last few years [12, 17–19]; however, almost all of them deal with even-even systems. In particular those made by Flaum and Cline [18] in connection with decoupled negative-parity bands in even-even rare earth nuclei show a decoupling behaviour very similar to that appearing here.

We have collected in fig. 8 data concerning the g.s.b. of ^{194,196}Hg [ref. [11])] (which represent the relevant cores for the Tl nuclei under discussion), the recently reported $\tilde{\pi}h_{\frac{9}{2}}$ bands in odd mass Tl isotopes [8]) and the now available information on the negative-parity bands in doubly odd ^{196,198}Tl [ref. [14])]. The odd-odd data have been redrawn in order to incorporate the prediction of the theory (see below). It must be stressed that such a possibility is fully consistent with all of our measurements. The parallelism between the two $\tilde{\pi}h_{\frac{9}{2}} \otimes \tilde{\nu}i_{\frac{13}{2}}$ bands in ^{198}Tl and ^{196}Tl (starting from the 122.2 and 108.6 keV γ-rays, respectively) is remarkable and therefore we are forced to admit that the transition in ^{198}Tl corresponding to the 61.5 keV γ-ray in ^{196}Tl was not detected (reasons for that are already given in the preceding section).

In fact, a careful examination of fig. 8 strongly suggests the way the explanation must go. In the following we want to discuss the three particular features displayed

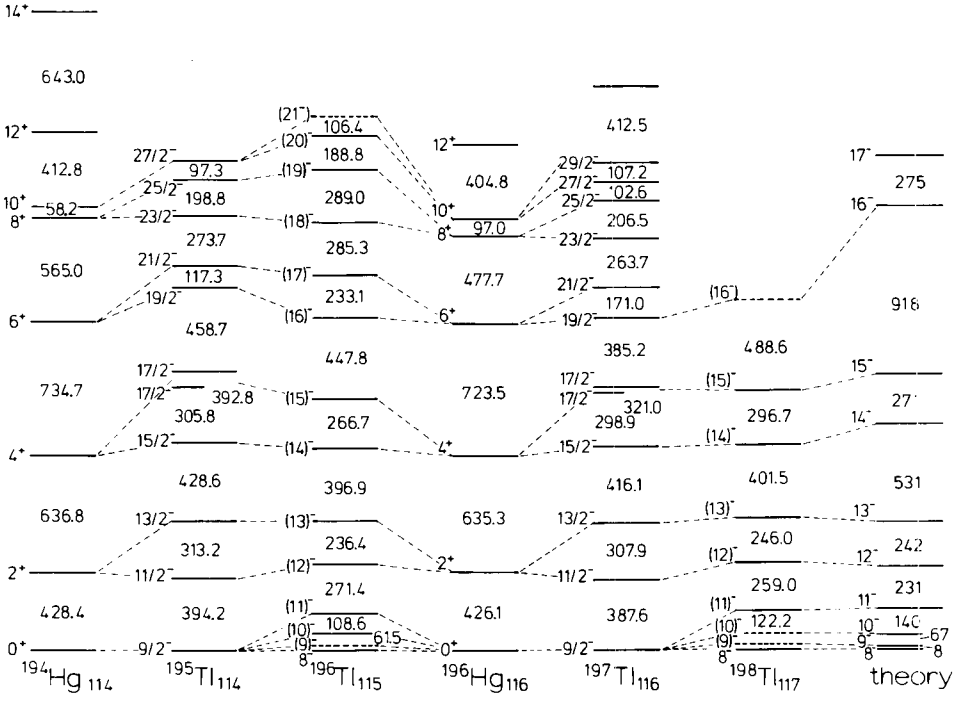

Fig. 8. Ground-state bands of ^{194,196}Hg [ref. [11])], $\tilde{\pi}h_{9/2}$ bands in ^{195,197}Tl [refs. [8, 9])] and $\tilde{\pi}h_{9/2} \otimes \tilde{\nu}i_{13/2}$ bands in ^{196,198}Tl.

by the doubly odd bands, namely: (i) the comparatively small initial transition energies, (ii) the odd-even staggering in the excitation energies and (iii) the compression of the levels above the $(17)^-$ level (from now on the state labels of fig. 8 are used).

In the present case the appropriate configuration space to describe the intrinsic motion turns out to be the product space $\tilde{\pi}h_{\frac{9}{2}} \otimes \tilde{\nu}i_{\frac{13}{2}}$ (for further details see ref. [14])). For Tl nuclei in the mass region under consideration the positions of the proton and neutron Fermi levels are so that quasiparticle excitations in the $\pi h_{\frac{9}{2}}$ subshell have predominantly particle character whereas $\tilde{\nu}i_{\frac{13}{2}}$ excitations are mainly holes. Moreover, this means, for oblate deformation, that the $\Omega_p = \frac{9}{2}$ state has the lowest excitation energy for the proton whereas for the neutron it is the state with the smallest projection ($\Omega_n = \frac{1}{2}$) on the symmetry axis which lies nearest to the Fermi surface. In this situation and for vanishing collective angular momentum (as it turns out to be) the orthogonal coupling of the two quasiparticles is the energetically most favourable configuration (which indeed gives $I = 8$). From now on the system has two different ways of gaining angular momentum. In a strong coupling situation it will start adding collective spin. In the present case, however, where the deformation is small and the adiabatic condition is not fulfilled it is energetically more convenient for the system to change the orientation of the particles. The projection of the neutron spin on the symmetry axis increases somewhat and the spin of the proton decreases so that they become more aligned with the total angular momentum and also with each other. This can be done up to spin 11, which is the highest possible value for the orbitals involved, without adding a significant amount of collective rotation. Hence the calculated quasidegeneracy of the 8^--11^- multiplet offers an explanation for point (i).

From here on the system starts to rotate. As may be seen in fig. 8 this coincides with the appearance of the staggering feature. This behaviour is already present in the $\tilde{\pi}h_{\frac{9}{2}}$ bands of neighbouring odd Tl isotopes and appears to be of the same magnitude. Such a similarity strongly suggests the same origin in both cases (this is indeed confirmed by calculations performed for the odd Tl case [20])). In fact, each level of the g.s.b. in the core nucleus gives rise to two yrast states of opposite signature [21]) in the odd spectrum (the signature quantum number will be taken as $(-1)^I$). Dashed lines connecting states are not just to guide the eye, they imply a real parentage between them. "Unfavoured" and "favoured" states (for instance $\frac{15}{2}^-$ and $\frac{17}{2}^-_1$ in odd Tl and $(14)^-$ and $(15)^-$ in doubly odd Tl) have essentially the same core angular momentum; they only differ by the orientation of $\boldsymbol{j}_{\text{prot}}$ relative to the total spin. The single addtional unit of angular momentum in the favoured states is obtained by tilting $\boldsymbol{j}_{\text{prot}}$ in order to give a larger projection on I. There is some problem here concerning the existence of two nearby lying $\frac{17}{2}^-$ states in the odd mass spectra but this feature is independent of the present discussion and will be taken up in a different publication [20]). The argument which led us to propose the presence of an additional unobserved low energy transition is *specifically* connected with the staggering phenomenon. In this point the statement made by the calculation is very conclusive:

the non-existence of this transition would imply that prediction and measurement are opposite in phase. This can be seen in fig. 8 where the theoretical results are shown in the last column [parameters of the calculation are: quadrupole deformation $= -0.13$, Nilsson parameters the same as in ref. [14]), Grodzins' value for the moment of inertia [14]), $\Delta_n \approx 0.8$ MeV and $\Delta_p \approx 0.9$ MeV.]

One also may see that the calculation is able to reproduce reasonably well the experiment up to spin 15^-, even though the $14^- \rightarrow 13^-$ spacing is somewhat too large. The $16^- \rightarrow 15^-$ transition is already greatly overestimated. As implied above the separation between neighbouring unfavoured (or favoured) states is predominantly determined by the core spectrum (they differ by two units of collective spin) and the disagreement just indicates that it is not allowed to represent this core by a rigid rotor (this follows already from an examination of the g.s.b.). On the other hand the favoured (I) $\rightarrow$ unfavoured ($I-1$) spacings are well described; they are essentially determined by the quasiparticle spectrum. This transition energy is of intrinsic nature because the only difference between the two states is the orientation of j_{prot}. Analytically, the separation of the rotational yrast states into two sequences of opposite signature appears to be related to the signature dependence of some non-diagonal Coriolis matrix elements arising from the interference of the "direct" and $\mathcal{R}$-reflected [21]) parts of the wave functions. Hence, the staggering can be understood as a specific quantal feature intimately connected with the reflection symmetry of the deformation.

Let us now come to the third feature. Above the 6^+ states in the mercury isotopes the g.s.b. deviate drastically from a quasirotational behaviour. The $8^+ \rightarrow 6^+$ spacing is already smaller than the $6^+ \rightarrow 4^+$ one and the 10^+ state lies very close to the 8^+. A new band starts on top of the 10^+ state resambling the initial g.s.b. This phenomenon has been repeatedly discussed by several authors [10,11,13]). In the lighter Hg isotopes ($A \leqq 196$) the discontinuity is believed to arise from the crossing of the g.s.b. by a two-quasiparticle aligned $\tilde{\pi}h^2_{\frac{11}{2}}$ band. The compression of the $\tilde{\pi}h_{\frac{9}{2}}$ band above the $\frac{19}{2}^-$ state has been recently interpreted as also reflecting the same structural change [8,9]). It is very likely that the same process is responsible for the pronounced quenching of the levels above the 16^- in ^{196}Tl. Further support comes from the dissapearance of the crossover transitions which indicates the reduction in collectivity in these states in analogy to the retardation of the $10^+ \rightarrow 8^+$ transition rates [13]). This will imply the interruption of the band in a completely aligned four-quasiparticle configuration: $[\tilde{\pi}(h_{\frac{9}{2}}h^2_{\frac{11}{2}}) \otimes \nu i_{\frac{13}{2}}]_{21-}$. The mass distribution generated and induced by such a configuration will represent a large triaxial disturbance on the originally axially symmetric oblate deformation. Moreover, these aligned high-j orbitals tend to produce an axially symmetric average field, but now around the rotation axis. Hence it seems that doubly odd Tl nuclei may be especially suited to study the transition between a quantal collective rotation around an axis perpendicular to the symmetry axis and a regime where the total spin is built up from many single-particle contributions and takes place around the symmetry axis of the system [22]).

Therefore the investigation of the 8^- band beyond the 21^- state would be very interesting.

We express our gratitude to R. M. Lieder, H. Beuscher, Y. Gono, D. Haenni and M. Müller-Veggian for their help during the irradiations at Jülich. One of us (A.J.K.) wants to acknowledge sincerely the hospitality of Prof. H. Morinaga and all members of the E17 Institute at the Technical University Munich and in particular the extremely efficient technical assistance of Miss U. Heim.

References

1) J. O. Newton, S. D. Cirilov, F. S. Stephens and R. M. Diamond, Nucl. Phys. **A148** (1970) 593
2) J. O. Newton, F. S. Stephens and R. M. Diamond, Nucl. Phys. **A236** (1974) 225
3) J. Meyer-ter-Vehn, F. S. Stephens and R. M. Diamond, Phys. Rev. Lett. **32** (1974) 1383
4) D. Proetel, D. Benson, Jr., A. Gizon, J. Gizon, M. R. Maier, R. M. Diamond and F. S. Stephens, Nucl. Phys. **A226** (1974) 237
5) P. O. Tjøm, M. R. Maier, D. Benson, Jr., F. S. Stephens and R. M. Diamond, Nucl. Phys. **A231** (1974) 397
6) H. Toki and A. Faessler, Nucl. Phys. **A253** (1975) 231
7) Y. Gono, R. M. Lieder, M. Müller-Veggian, A. Neskakis and C. Mayer-Böricke, Phys. Rev. Lett. **37** (1976) 1123
8) R. M. Lieder, in Proc. Int. Symp. on collectivity of medium and heavy nuclei, Tokyo, 1976, ed. Y. Shida, p. 459
9) R. M. Lieder, A. Neskakis, M. Müller-Veggian, Y. Gono, C. Mayer-Böricke, S. Beshai, K. Fransson, C. G. Linden and Th. Lindblad, to be published
10) D. Proetel, R. M. Diamond and F. S. Stephens, Nucl. Phys. **A231** (1974) 301
11) R. M. Lieder, H. Beuscher, W. F. Davidson, A. Neskakis and C. Mayer-Böricke, Nucl. Phys. **A248** (1975) 317
12) F. S. Stephens, Rev. Mod. Phys. **47** (1975) 43, and references therein
13) C. Günther, H. Hübel, A. Kleinrahm, D. Mertin, B. Richter, W. D. Schneider and R. Tischler, Phys. Rev. **C15** (1977) 1298
14) A. J. Kreiner, M. Fenzl, S. Lunardi and M. A. J. Mariscotti, Nucl. Phys. **A282** (1977) 243
15) R. Brings, G. Lürken and P. Wucherer, Annual Report IKP, KFA Jülich (1975) 248
16) Nucl. Data Sheets, Nuclear level schemes $A = 45$ through $A = 257$ (Academic Press, NY, 1973)
17) K. Neergård, P. Vogel and M. Radomski, Nucl. Phys. **A238** (1975) 199
18) C. Flaum and D. Cline, Phys. Rev. **C14** (1976) 1224
19) H. Toki, H. L. Yadav and A. Faessler, Phys. Lett. **66B** (1977) 310
20) A. J. Kreiner, to be published
21) A. Bohr and B. R. Mottelson, Nuclear structure, vol. 2 (Benjamin, NY, 1975)
22) A. Bohr and B. R. Mottelson, Physica Scripta **10A** (1974) 13